Heliyon 9 (2023) e13197

Contents lists available at ScienceDirect

Heliyon

journal homepage: www.cell.com/heliyon

Research article

Catalog of 525 sprites observed over Japan from September 2016 to March 2021

Maomao Duan [a,*], Takanori Sakamoto [a], Teruaki Enoto [b], Yuuki Wada [c,b], Masashi Kamogawa [d], Koji Ito [e]

[a] Department of Physical science, Aoyama Gakuin University, Sagamihara City, Kanagawa Prefecture, Japan
[b] Extreme Natural Phenomena RIKEN Hakubi Research Team, Cluster for Pioneering Research, RIKEN, Saitama, Japan
[c] Division of Electrical, Electronic and Infocommunications Engineering, Graduate School of Engineering, Osaka University, Osaka, Japan
[d] Natural Disaster Research Section, Global Center for Asian and Regional Research, University of Shizuoka, Shizuoka, Japan
[e] SonotaCo Network, Japan

ARTICLE INFO

Keywords:
Sprite
Transient luminous events
Lightning

ABSTRACT

We present a catalog of 525 sprites detected over the Sea of Japan and a northeast part of the Pacific Ocean from Sagamihara between September 2016 and March 2021. We analyze the morphology of 525, estimate the location of 441, and calculate the accurate top height of 15 sprites. More than half of our samples occurred in winter, while only 11% were in summer. In terms of morphology, 52% to 60% column type sprites took place in spring, autumn, and winter, while only 15.5% in summer. Therefore, summer thunderstorms are more likely to produce sprites with complex structures like carrots. Furthermore, sprites in summer are almost all located on the main island of Japan, and their spatial distributions are significantly different from the other seasons. Finally, from the perspective of the time distribution, the number of sprites is the largest at 1:00 JST. In addition, the morphology of sprites tends to be simple (e.g., a column type) at midnight JST.

1. Introduction

Thunderclouds produce optical emission phenomena such as blue jets, blue starters, sprites, elves, and giant jets [2,44]. These phenomena are collectively called transient luminous events (TLEs). The height of TLEs is 20 - 100 km [38,48,52,13,19,11,45]. Sprites are the most frequently observed TLEs from the ground. Sprites are a luminescence phenomenon occurring in the middle atmosphere about 60 to 90 km and are high-rise discharges. Their color is red due to several excitation states of molecular nitrogen [20,31], and they appear for a short period of ~1 ms [40,4]. The Quasi-Electrostatic (QE) model is a general physical mechanism of the sprite [37,36]. According to the QE model, a quasi-static electric field is applied at an altitude above the cloud due to a positive lightning strike. The quasi-static electric field accelerates electrons. The accelerated electrons collide with the neutral atmosphere and the collisions cause de-excitation to produce a flash of light. In previous reports, since the proportion of negative sprites is less than 0.1%, it is generally believed that a positive polarity discharge causes sprites [10]. However, recent studies have found that the proportion of sprites caused by a negative polarity discharge can reach ~18% [25,28] or even ~25% [10].

* Corresponding author.
E-mail address: mdan@phys.aoyama.ac.jp (M. Duan).

https://doi.org/10.1016/j.heliyon.2023.e13197
Received 6 July 2022; Received in revised form 16 January 2023; Accepted 20 January 2023

Available online 17 February 2023

Fig. 1. The cameras of ASCA installed on the roof of the Sagamihara campus, Aoyama Gakuin University, Japan.

Based on the optical observation data, the morphologies of sprites are typically a column or a carrot type [42,53,8]. Less common morphologies include angel type, firework type, and dancing type [29,47,8]. In addition, the morphology of sprites varies in different regions and seasons. For example, according to Hayakawa [16] observations in the winter of 2001/2002, 26 sprites were observed in the Hokuriku area of Japan, of which 25 were of the column type, and only one was a carrot type. In addition, Adachi [1] classified 67 sprites observed in 5 winters between 1998 and 2003. There are 38 column types and eight carrot types, and the remaining 21 sprites are not classified because trees or mountains occlude the images of these sprites. However, summer sprites on the American continent are very different and more complex in morphology [1,16,17,35,49]. Also, Asano et al. [3] noticed that summer sprites in Japan are more complex than winter sprites, with carrot type being the majority. But since the samples are still small in their studies, more evidence is needed to obtain a concrete picture of sprites in Japan.

Sprites might contribute to important greenhouse gases such as ozone and nitrous oxide (N_2O). The latest laboratory studies show that streamers in laboratory corona discharges produce a non-negligible amount of O_3 and N_2O [14,15]. Therefore, as climate concerns become more prominent, accurate measurements of the sources of N_2O are necessary. It is also important to explore the role of sprites in the global chemical atmosphere [15].

Here we present a catalog of 525 sprites, an unprecedented dataset of sprites detected over Japan. Their quantity, morphology, spatial distribution, and top height are analyzed and discussed.

2. Instrumentation

In September 2016, we installed three wide-field optical cameras called Aoyama Gakuin University Sprite Camera (ASCA) on the roof of the Sagamihara campus, Aoyama Gakuin University, Japan (N35.57°, E139.40°). The device consists of a CCD camera (Watec WAT-902H2 ULTIMATE), an f 2.9-8 mm camera lens (Fujinon varifocal lens), and a rainproof camera housing. The field of view of the camera is 33.4° × 43.6°. The vertical angle is 33.4° and the horizontal angle is 43.6°. The three cameras are facing north, northeast, and west from the location (Fig. 1). The analog output from the camera connects to an analog video capture device (Buffalo PC-SDVD/U2G), which captures frames at approximately 30 fps. The captured frames are processed on a PC by the software UFOCaptureV2[1] [32,50] in real-time. When the UFOCaptureV2 identifies a possible TLE by examining the difference between a previous frame and a current frame, the software records frames around the trigger time for three seconds (one second before the trigger time and two seconds after the trigger time) on the PC. The time on the PCs was synchronized by the NTP server of the university every 600 s. However, we introduced the GPS module to obtain a high accuracy time in November 2019. The observation starts automatically from sunset to sunrise every day.

3. Analysis & results

By March 2021, ASCA detected a total of 525 sprites. The morphology of 525 sprites was classified by eye inspection. We used UFOAnalyzerV2[2] [33,9] for the analysis of the locations of sprites. First, we created the camera profile file by correlating the position

[1] https://sonotaco.com/soft/UFO2/help/english/index.html.
[2] https://sonotaco.com/soft/download/UA2Manual_EN.pdf.

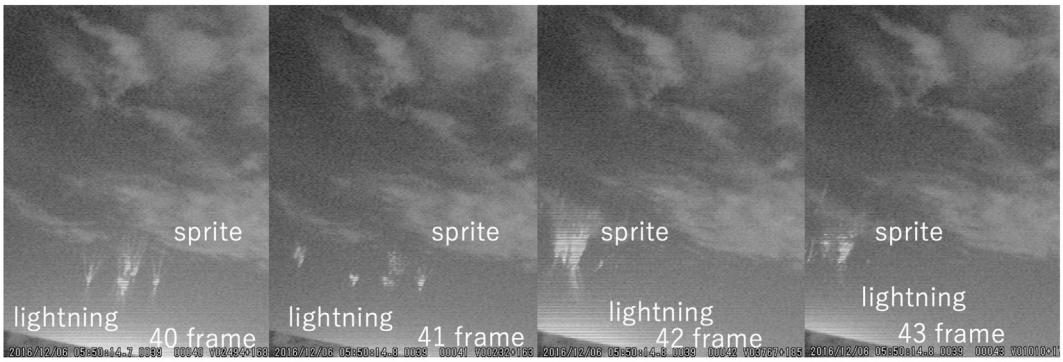

Fig. 2. The frame-by-frame images of the sprite observed at 05:50:14 on December 06, 2016 JST. The sprite appeared with the lightning in the 40th frame, and another sprite happened in the 42nd frame.

of the observed stars to the bright star catalog. UFOAnalyzerV2 uses the camera profile file to calculate the azimuth and elevation of the events. Second, assuming the top height of sprites is 80 km, UFOAnalyzerV2 estimates the location of sprites. Sometimes several sprites appear continuously in a single recorded video, as shown in Fig. 2. UFOCaptureV2 uses the automatically captured image for the location analysis of sprites, which is usually the first detected sprite. And other sprites that appear in the later frames are not often identified as individual events by UFOCaptureV2. Therefore, we only analyzed the location of the first sprite in the recorded video. The total number of sprites with the location analysis is 441. Appendix A summarizes the sprites observed during the approximately five years from September 2016 to March 2021. Table 1 records the basic information of sprites, including the detection time in JST, location, and morphology. SpriteAnalyzerV2[3] is a triangulation tool that calculates the latitude, longitude, and altitude of sprites precisely from the azimuth and the elevation of multiple sites. For 15 sprites, SpriteAnalyzerV2 calculated the top height of sprites and location using triangulation. The summary of the triangulation analysis is described in appendix B of Table 2.

3.1. Seasonal and daily variation of sprites

The morphology of sprites is divided into four types: column type, carrot type, multiple type, and other types (Figs. 3(a - d)). The classification results are summarized for each camera and the sum of all cameras in Figs. 4(a - d). As a result of classification, the column type was the most common (~50%). There was no substantial difference in the morphology of sprites detected by the individual cameras (Figs. 4(a - d)). In addition, according to the classification of different seasons (Figs. 5(a - d)), the proportion of column type in spring (from March to May), autumn (from September to November), and winter (from December to February) is more than 50%, whereas only 15.5% in summer (from June to August). Thus, the fraction of the column type in summer is significantly smaller than in other seasons. When we compare the total numbers of sprites between winter and summer, ASCA detected 272 sprites during winter. But only 58 sprites were observed in summer. Although our camera system is not covering the entire area of Japan, a seasonal difference in the occurrence rate of sprites is evident in our ASCA samples.

As shown in Fig. 6, the most significant number of sprites were detected at midnight (1:00 JST), corresponding to 15.8% of the total sample. On the other hand, the smallest number of sprites were seen around sunrise and sunset. According to the morphology, the column type was the most at midnights, such as 66.3% and 76.5% at 1:00 and 2:00 JST. No column type was observed at 17:00 and 18:00 JST (sunset), and a small fraction of a column type was seen at 6:00 JST (sunrise).

3.2. Location of sprites

First, we generated the camera profile file for each camera to match the bright stars in the background of an individual frame to the stars in the SKY2000 Star Catalog [34] using UFOAnalyzerV2. Second, the software calculates an azimuth, an elevation, and a rotation angle of the event using the camera profile file. Finally, the location of a sprite determines, assuming the top height is 80 km. Fig. 7 shows the locations of 441 sprites. From the overall distribution map of Fig. 7, most sprites concentrated on the coast of the Sea of Japan. However, sprites were distributed on the pacific ocean too. The sprites' locations in different seasons are shown in Fig. 8. The location distribution of summer sprites is different from other seasons, and their locations are almost all located on Japan's main island. But, the sprites are distributed not only on Japan's main island but also on the Sea of Japan and the Pacific Ocean in other seasons.

3.3. Triangulation of sprites

We collaborated with the observers of the SonotaCo Network to analyze the same sprites observed in the different sites to obtain an accurate latitude, longitude, and top height. Our synchronization criteria are the sprite coincides, the sprite morphology is almost

[3] http://sonotaco.com/soft/SA2/SA2.html.

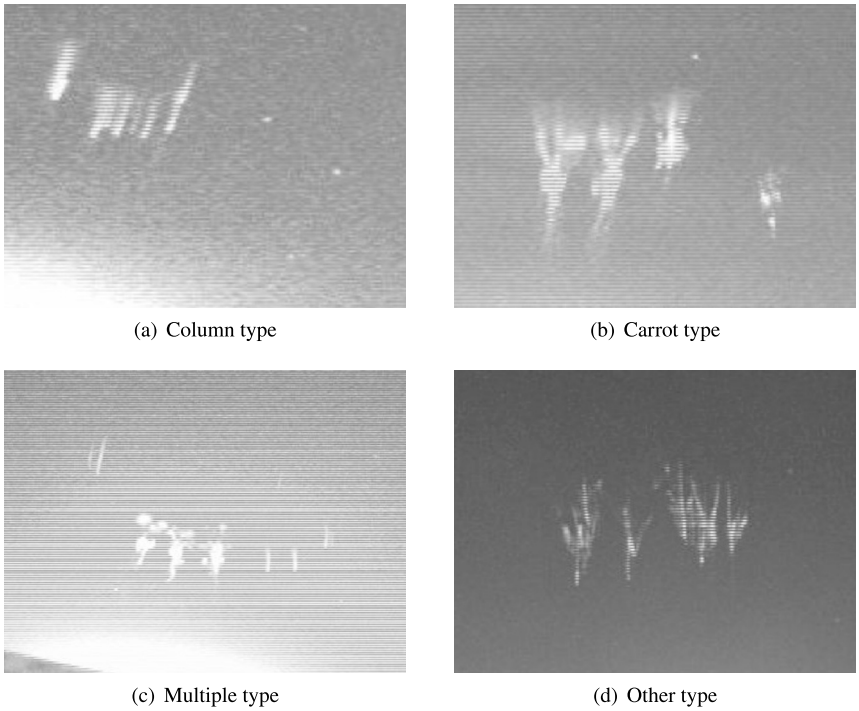

(a) Column type (b) Carrot type

(c) Multiple type (d) Other type

Fig. 3. Classifications of sprites in four different types.

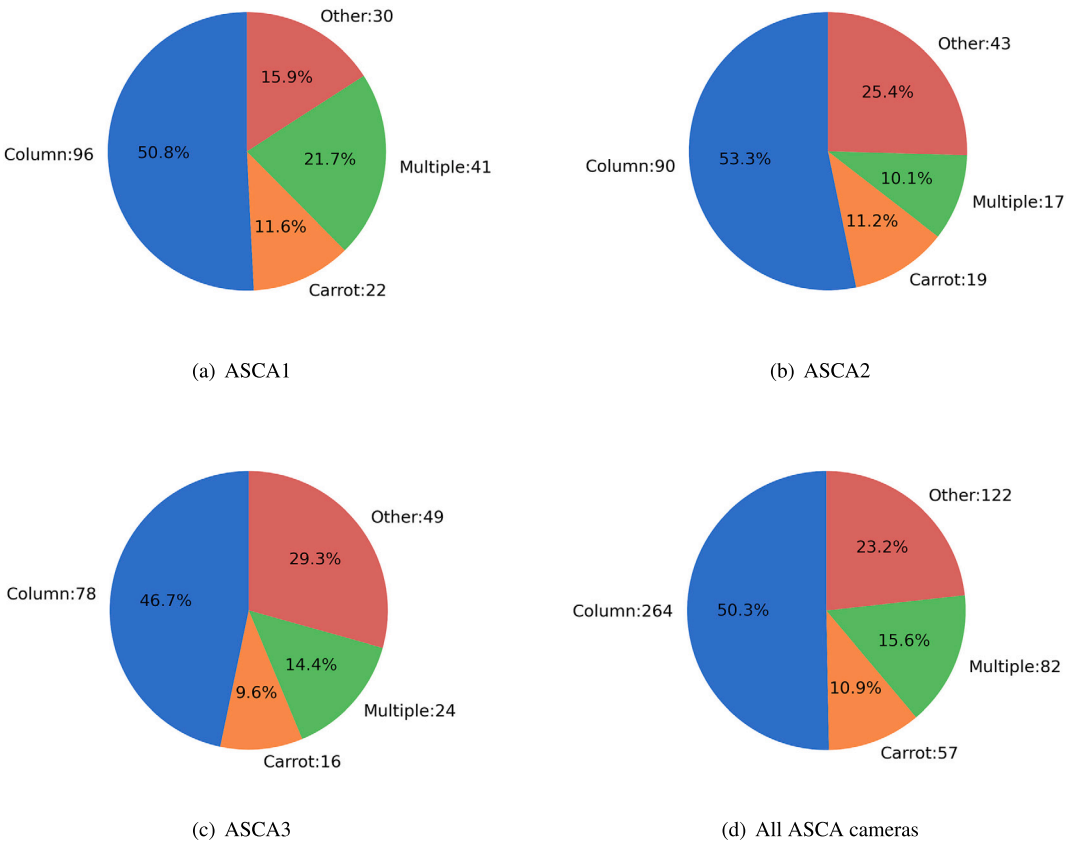

(a) ASCA1 (b) ASCA2

(c) ASCA3 (d) All ASCA cameras

Fig. 4. The morphological distributions of the observed sprites by the individual cameras and the all cameras.

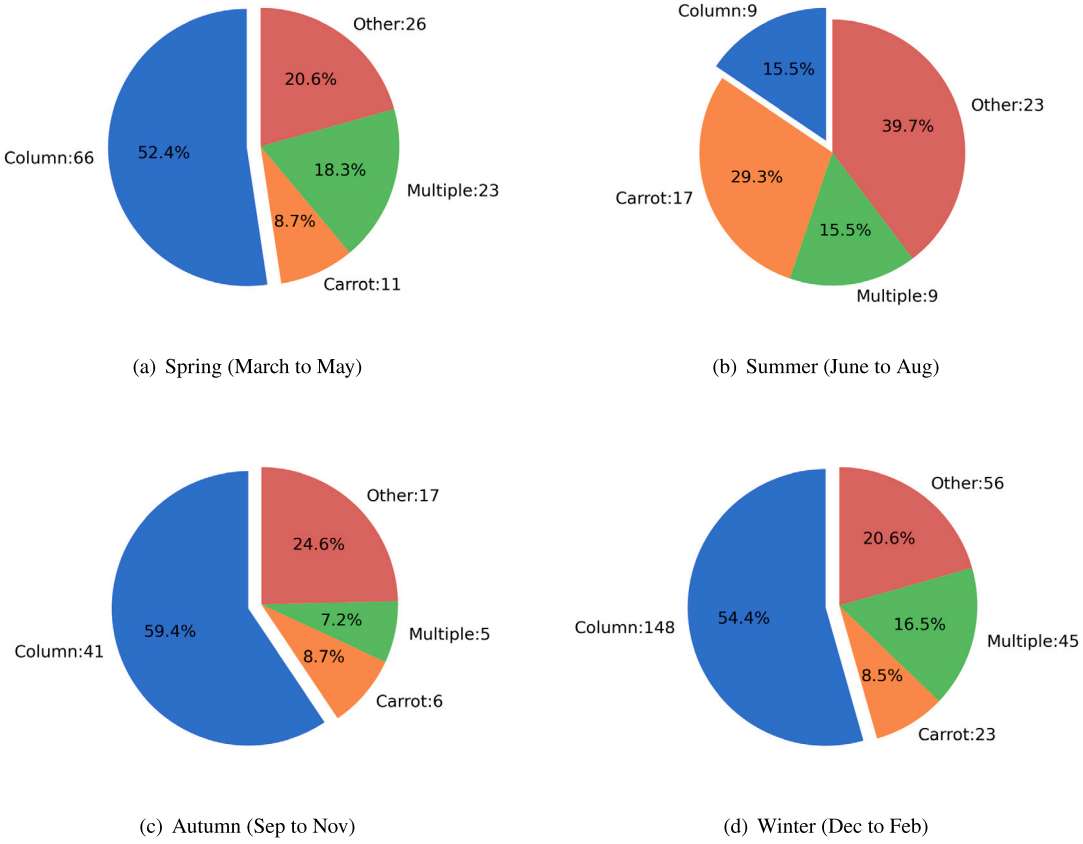

(a) Spring (March to May) (b) Summer (June to Aug)

(c) Autumn (Sep to Nov) (d) Winter (Dec to Feb)

Fig. 5. The seasonal distributions of the observed sprites in four seasons.

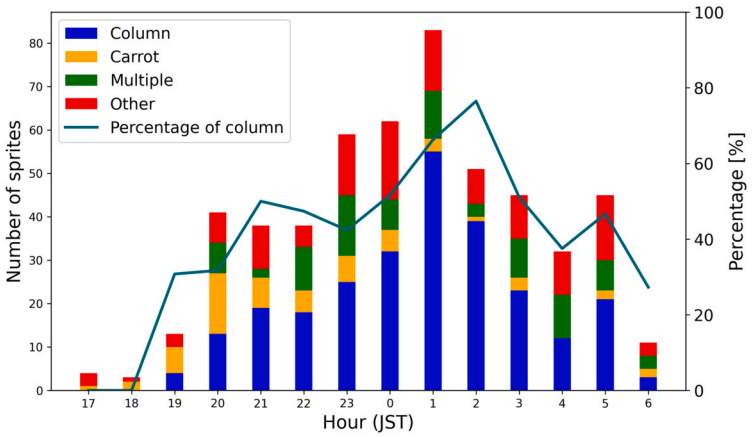

Fig. 6. Hourly distribution of sprites. The blue bar is column type, the orange bar is carrot type, the green bar is multiple type, and red bar is other type. The line shows the percentage of the column type over the total number of sprites for each hour.

the same, and the estimated location of the sprite by an individual analysis is close to each other. As a result, there were about 60 sprites. Because the crossing angles were less than 5 degrees or challenging to confirm the correspondence of each part of the sprites, we analyzed 15 of them. Since a single sprite event could include several components, the total parts for the analysis were 58 elements. For example, on March 24, 2018, the ASCA1 and the camera in Tokyo (N35.66°, E139.67°) detected the same sprite and analyzed it with SpriteAnalyzerV2. As shown in Fig. 9, the multiple elements of the sprite were distributed in the range of 34 - 52 km. Out of the 58 elements, 49 were columns, 2 were carrots, and 7 were other types. And the average top height of sprites was 82 ± 4 km. There was no tendency for the top height to vary due to a morphology of a sprite. Therefore, it is reasonable to assume that the sprites' top height is 80 km when estimating the sprite location.

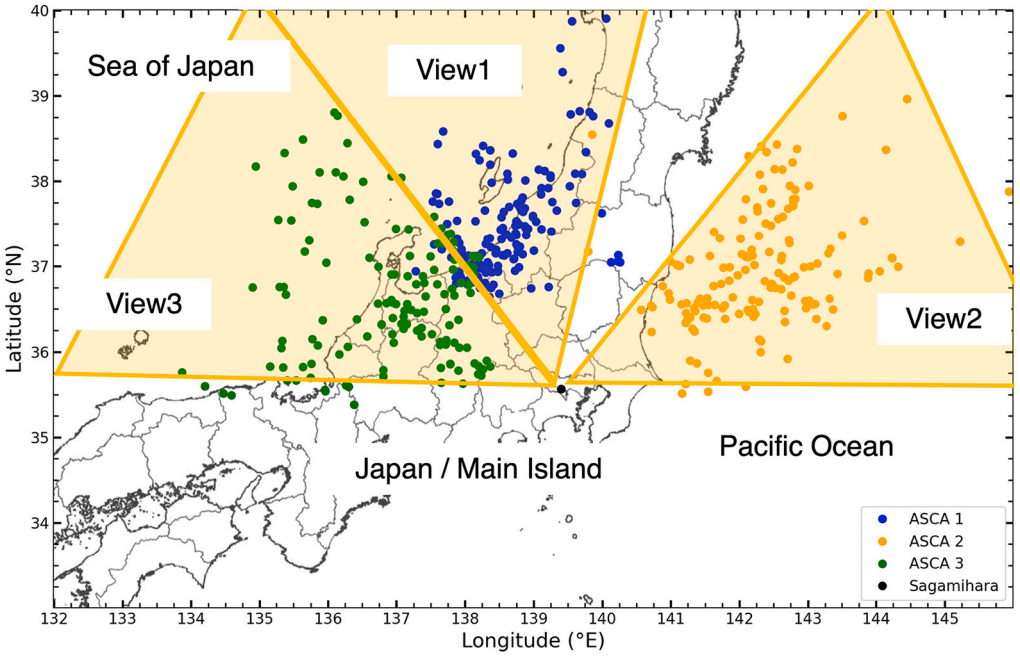

Fig. 7. A location map of 441 sprites from December 2016 to March 2021 by the different ASCA cameras. The different colors correspond to the sprites detected by ASCA1 (blue), ASCA2 (yellow) and ASCA3 (green). The hatched areas show the field of view of each ASCA camera in March 2021. Some of the sprites were not in the field of view because ASCA orientation differed in the early testing phase. And also, the orientation changed significantly due to the strong wind (e.g., typhoons). The background map is provided by Geospatial Information Authority of Japan.

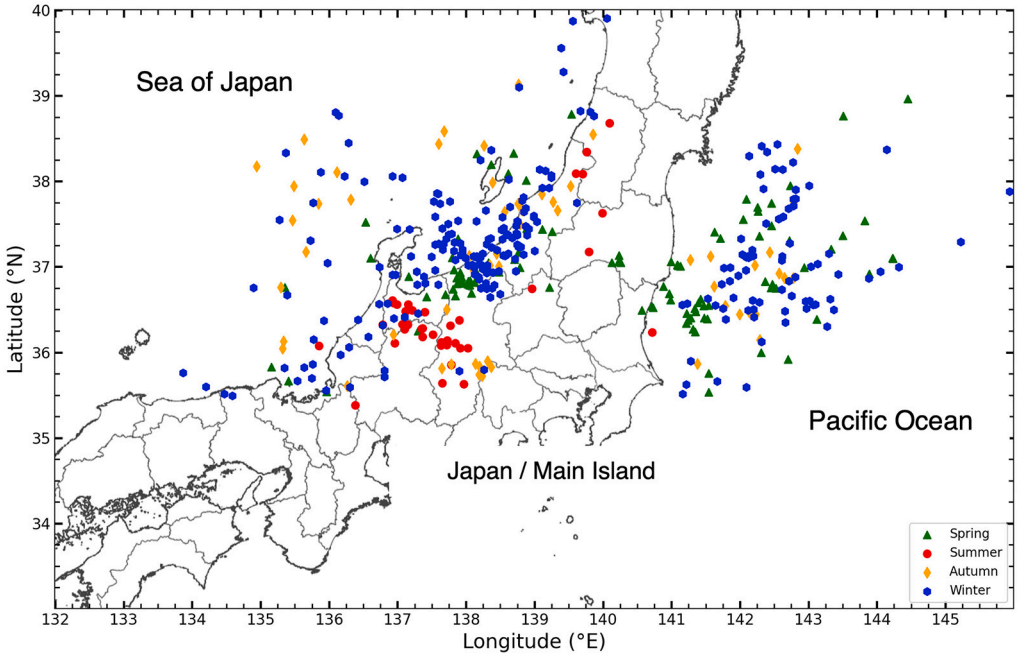

Fig. 8. A location map of 441 ASCA sprites from December 2016 to March 2021 in different seasons. Spring, summer, autumn and winter are represented by green triangles, red dots, yellow diamonds, and blue hexagons, respectively. The background map is provided by Geospatial Information Authority of Japan.

In addition, triangulation can accurately calculate the sprite location with very little uncertainty [26,30,54]. However, the systematic error in the location is unclear, assuming a top height of a sprite to be 80 km. Using the triangulated samples, we estimate the systematic difference in the location of sprites using the accurate top height and the assumed height of 80 km. Fig. 10 compares the location obtained by the triangulation and the location obtained by the estimation. The average distance difference between the locations calculated by the two methods is 9 ± 6 km. The error is calculated as the standard deviation of the differences.

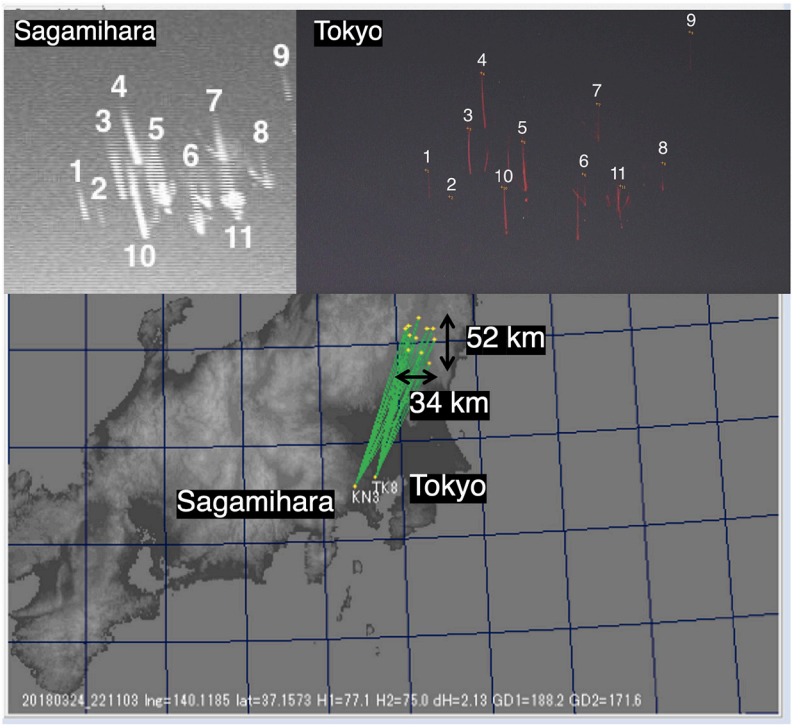

Fig. 9. Results of triangulation of the sprites observed at 22:11:03 on March 24, 2018 JST using SpriteAnalyzerV2. The upper figures show the sprite images of ASCA1 (labeled as Sagamihara) and the camera of the Tokyo (N35.66°, E139.67°) site. The bottom figure shows the distribution of each part of the sprite on the map.

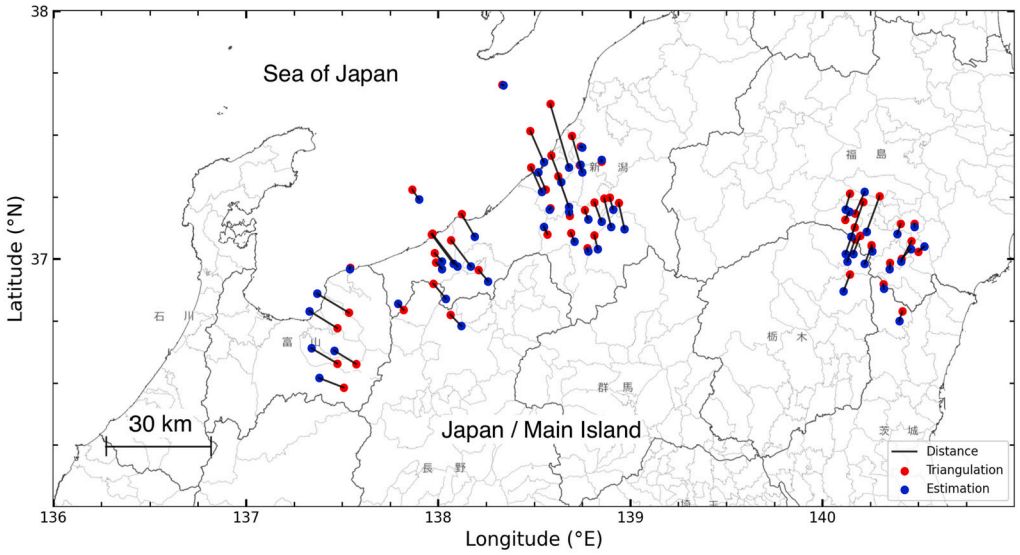

Fig. 10. The triangulated (red) and the estimated (blue) locations of sprites. The background map is provided by Geospatial Information Authority of Japan.

One of the conclusions about the significant difference in the distribution of sprites in summer (Fig. 8 of §3.2) is still valid taking into account this uncertainty.

4. Discussion

The observed sprites in summer are significantly less than in winter (Figs. 5(a - d)). For example, from September 2016 to March 2021, the number of sprites per summer and winter is 14.5 and 54.4. According to the QE theory, a positive cloud-to-ground strike

(+CG) causes sprites [37,36]. In Japan, cloud-to-ground strikes (CGs) in summer are an order of magnitude more than in winter [41,43]. But +CGs occur only about 10% in summer, and about 50% in winter [35,49]. And the +CGs in winter can transfer an enormous amount of charge [7,35,49]. Therefore, the +CGs with a hefty charge amount transferred in winter are more than in summer. That's why many winter sprites were observed on the Hokuriku of Japan, and summer sprites are scarce [16]. However, sprites are not necessarily all related to +CGs. A few sprites are generated by -CGs [5,6,21–24,27,51]. Although previous studies proved a positive polarity of winter sprites on the Hokuriku and the coast of the Sea of Japan [1,16,49], the polarity of summer sprites is unclear. Previously, sprites were generally considered to be associated with +CGs, as only 22 cases were negative sprites [10]. But in recent years, Lu et al. [25,28] investigated lightning strikes associated with sprites observed by the Imager of Sprites and Upper Atmospheric Lightning (ISUAL) in North America. The results showed that the percentage of negative sprites was about 18%. And they are usually accompanied by halos, which occur mainly in oceanic and coastal thunderstorms. Therefore negative sprites are more likely to be generated in marine areas. According to Chen et al. [10], sprites observed by the ISUAL mission contained 127 negative sprites, accounting for ~25% of all the polarity identified sprites. Furthermore, unlike Lu et al. [25,28], Chen et al. [10] suggested that the polarity of sprites is latitude-dependent. Negative sprites mainly congregate in the latitudinal regions below 20°, while positive sprites scatter up to 50°. Although the ASCA sprites have a higher latitude, greater than 35°, it is inappropriate to speculate that the polarity of sprites is all positive. Another point is that negative sprites are more likely to appear in the sea and areas close to the ocean, which fits Japan's geography. To explain why there are fewer summer sprites than winter sprites, a combination of lightning observation data is needed to understand the polarity of summer sprites.

Our classification shows that the morphology of sprites in spring, autumn, and winter is relatively simple, and more than half of them are column types. On the other hand, the morphology of summer sprites is more complex. Only 15.5% of them are column types (Figs. 5(a - d)). Previous studies have shown that the morphology of winter sprites in the Hokuriku and the coast of the Sea of Japan is simpler than summer sprites in the American continent [1,16–18]. Asano et al. [3] suggested that summer sprites in Japan are mainly carrot types based on their limited samples. The simulation [3] showed that the height of lightning discharge, charge amount transferred, and lightning current rise time are closely related. The altitude of thunderclouds in summer is about 10 km, whereas a few kilometers in winter. Therefore, the height of the charge is the essential parameter between summer and winter lightning. If the altitude of a lightning discharge is higher, sprites have a complex structure, such as the carrot type. Therefore, more complex sprites exist in summer. Contreras-Vidal et al. [12] suggests that the morphology of sprites is related to the lightning peak current, and the peak current of the column type is smaller than that of the carrot type. In addition, as the peak current value increases, the morphology of the sprites becomes more complex. In addition, Qin et al. [39] points out in the simulation that the electron number density of the ionosphere will affect the morphology of sprites. The triggering condition of the carrot type is stricter than that of the column type. However, when the electron number density decreases, the carrot type becomes more likely to appear.

As shown in Fig. 6, sprites are more abundant at midnight and less numerous at sunrise and sunset. There are two possible reasons. First, capturing sprites with optical cameras is not easy due to the bright sky around sunrise and sunset. Second, due to the high density of electrons, it is not conducive to generate sprites. As Stanley et al. [46] suggested, the high density of electrons in sprites during the day makes it challenging to meet the relaxation time required for producing sprites. Therefore, to meet the condition of relaxation time, it is necessary to reduce the occurrence height of sprites. Unfortunately, as the altitude decreases, the density of air increases and the threshold for electrical breakdown also increases, which is unfavorable for the occurrence of sprites. In addition, the morphology of sprites at sunrise and sunset is more complex, and the column type accounts for a small proportion. The reason may also be related to the ionospheric environment. However, due to the small number of sprites at sunrise and sunset, more data are needed to prove that the sprites at sunrise and sunset have more complex morphology.

The geographic distribution of summer sprites is significantly different from other seasons. Almost all of them are concentrated on Japan's main island (Fig. 8) and have been noticed in previous studies. For example, the lightning flash density map from Shindo et al. [43] shows that summer lightning in Japan is mainly concentrated on Japan's main island. This indicates that updrafts are more likely to form on land than in marine areas with high summer temperatures and create thunderclouds that trigger sprites when CGs occur.

5. Conclusion

We compiled 525 sprites observed during the approximately five years from September 2016 to March 2021 by ASCA. We found that there are many sprites in the Pacific Ocean, which have not received much attention before. In terms of the numbers, summer sprites are the least numerous, with 58 events (14.5 per season). Winter is the most, with 272 events (54.4 per season). Spring and autumn are somewhere in between. Morphologically, only 15.5% of the sprites are columns in summer, while more than half of the sprites in other seasons are columns. This suggests that summer sprites are not as simple in structure as sprites in other seasons. In the spatial distribution, summer is also obviously different from other seasons, and summer sprites are almost all concentrated on Japan's main island. Finally, from the perspective of time distribution, the number of sprites is the largest at 1:00 JST, accounting for 16% of the total sprite. In addition, the morphology of sprites tends to be simple around midnight JST.

Funding statement

Duan Maomao was supported by JST SPRING [Grant Number JPMJSP2103].

Table 1
Summary of sprites observed by ASCA. The complete data is available in the electrical form (OBJ_ASCA_Japan.csv).

date	lng1	lat1	frame	morphology
20161206_044208.0	137.594772	36.792366	32	column
20161206_052526.9	136.967819	36.907352	31	column
20161206_053223.6	137.098999	36.412266	31	column
20161206_053242.4	138.090164	37.023296	31	column
20161206_053247.6	137.176331	37.440285	31	column
20161206_053247.6			32	other
20161206_053513.5	136.855774	36.569302	31	column
20161206_053622.2	137.068527	38.045685	31	other
20161206_054139.3	136.780441	36.317688	31	column
20161206_054208.6	138.211319	37.029102	31	other
.....				

CRediT authorship contribution statement

Maomao Duan; Takanori Sakamoto: Conceived and designed the experiments; Performed the experiments; Analyzed and interpreted the data; Contributed reagents, materials, analysis tools or data; Wrote the paper.

Teruaki Enoto; Yuuki Wada; Masashi Kamogawa: Analyzed and interpreted the data; Contributed reagents, materials, analysis tools or data.

Koji Ito: Contributed reagents, materials, analysis tools or data.

Declaration of competing interest

The authors declare no competing interests.

Data availability

Data included in article/supp.material/referenced in article.

Acknowledgements

We would like to thank SonotaCo, the founder of the observation network. We also would like to thank the anonymous referees for comments and suggestions that materially improved the paper. This work was supported by JST SPRING, Grant Number JPMJSP2103.

Appendix A. Summary of sprites observed by ASCA

Table 1 lists sprites observed by ASCA over the last five years. 525 sprites are included in the table. The first column, date, is the recorded time of the sprite in *yyyymmdd_HHMMSS.S* format in JST, where *yyyy* is year, *mm* is month, *dd* is day, *HH* is hour, *MM* is minute, and *SS.S* is second. The next two columns, lng and lat, give a longitude and a latitude of the estimated sprite locations. East is positive in the longitudinal direction. North is positive in the latitudinal direction. A sprite with a blank lng and lat appears in the same video as the previous sprite, but not in the same frame and in a different location. The next column, frame, shows the frame number of the first frame when the sprite is detected. The next column, morphology, describes the morphology of the sprite.

Appendix B. Summary of the sprites observed by multiple locations

Table 2 shows the analysis results of sprites observed by multiple sites. 58 sprite elements are included in the table. The first column (date_seg) is the recorded time of the sprite and the segment number in *yyyyddmm_HHMMSS_NN* format, where *yyyy* is year, *mm* is month, *dd* is day, *HH* is hour, *MM* is minute, and *SS* is second in JST. *NN* is the segment number of the event. The next two columns (lng_d and lat_d) show the triangulated longitude and latitude of the sprites. East is positive in the longitudinal direction. North is positive in the latitudinal direction. The next column (h1_d) describes the triangulated height of the sprite. The next two columns (lng_p and lat_p) specify the estimated longitude and latitude of the sprites assuming the height of 80 km. The next column (morphology) shows the morphology of the sprite. The last column (distance) describes the difference in the distance in km between the triangulated (lng_d and lat_d) and the estimated (lng_p and lat_p) location.

Table 2
Parameters of the sprite's elements observed at multiple locations. The complete data is available in the electrical form (Sprite's_segments.csv).

date_seg	lng_d	lat_d	h1_d (km)	lng_p	lat_p	morphology	distance
20170103_022804_01	137.965302	37.099609	87.494934	138.08	36.98	column	16.75
20170103_022804_02	138.210342	36.955975	83.84201	138.26	36.91	column	6.75
20170103_022804_03	138.121857	37.180504	84.36982	138.19	37.09	column	11.74
20170103_022804_04	137.864609	37.280365	81.227493	137.9	37.24	column	5.47
20170103_022840_01	137.820099	36.794662	78.33345	137.79	36.82	column	3.89
20170103_022840_02	138.06398	36.775021	83.401718	138.12	36.73	column	7.07
20170103_022840_03	137.975021	36.900139	82.917061	138.04	36.84	column	8.84
20170103_022840_04	137.9879	36.986767	82.632889	138.02	36.96	column	4.12
20170103_022840_05	137.981476	37.023262	82.535858	138.02	36.99	column	5.04
20170103_022840_06	137.541367	36.965069	76.867874	137.54	36.96	column	0.58
20180324_215139_01	140.167572	37.127792	85.03685	140.12	37.02	other	12.71
20180324_215139_02	140.463867	37.072781	82.432571	140.41	36.99	other	10.37
20180324_215832_01	140.143646	37.262924	80.773323	140.12	37.2	column	7.3
20180324_215832_02	140.212967	37.229305	86.721443	140.15	37.09	column	16.46
20180324_215832_03	140.197464	37.093231	81.832603	140.16	37.02	column	8.8
20180324_215832_04	140.255753	37.05624	78.685989	140.26	37.03	column	2.94
20180324_215832_05	140.352112	36.985142	79.20134	140.35	36.96	other	2.8
20180324_215832_06	140.412704	37.001099	75.169167	140.46	37.04	column	6.03
.....							

References

[1] T. Adachi, Characteristics of thunderstorm systems producing winter sprites in Japan, J. Geophys. Res. 110 (2005), https://doi.org/10.1029/2004jd005012.

[2] E. Arnone, J. Bór, O. Chanrion, V. Barta, S. Dietrich, C.F. Enell, T. Farges, M. Füllekrug, A. Kero, R. Labanti, A. Mäkelä, K. Mezuman, A. Odzimek, M. Popek, M. Prevedelli, M. Ridolfi, S. Soula, D. Valeri, O. van der Velde, Y. Yair, F. Zanotti, P. Zoladek, T. Neubert, Climatology of transient luminous events and lightning observed above Europe and the Mediterranean Sea, Surv. Geophys. 41 (2019) 167–199, https://doi.org/10.1007/s10712-019-09573-5.

[3] T. Asano, M. Hayakawa, M. Cho, T. Suzuki, Computer simulations on the initiation and morphological difference of Japan winter and summer sprites, J. Geophys. Res. Space Phys. 113 (2008) A02308, https://doi.org/10.1029/2007ja012528.

[4] C.P. Barrington-Leigh, U.S. Inan, M. Stanley, Identification of sprites and elves with intensified video and broadband array photometry, J. Geophys. Res. Space Phys. 106 (2001) 1741–1750, https://doi.org/10.1029/2000ja000073.

[5] C.P. Barrington-Leigh, U.S. Inan, M. Stanley, S.A. Cummer, Sprites triggered by negative lightning discharges, Geophys. Res. Lett. 26 (1999) 3605–3608, https://doi.org/10.1029/1999gl010692.

[6] L.D. Boggs, N. Liu, M. Splitt, S. Lazarus, C. Glenn, H. Rassoul, S.A. Cummer, An analysis of five negative sprite-parent discharges and their associated thunderstorm charge structures, J. Geophys. Res., Atmos. 121 (2016) 759–784, https://doi.org/10.1002/2015jd024188.

[7] M. Brook, M. Nakano, P. Krehbiel, T. Takeuti, The electrical structure of the hokuriku winter thunderstorms, J. Geophys. Res. 87 (1982) 1207, https://doi.org/10.1029/jc087ic02p01207.

[8] J. Bór, Optically perceptible characteristics of sprites observed in Central Europe in 2007–2009, J. Atmos. Sol.-Terr. Phys. 92 (2013) 151–177, https://doi.org/10.1016/j.jastp.2012.10.008.

[9] J. Bór, Z. Zelkó, T. Hegedüs, Z. Jäger, J. Mlynarczyk, M. Popek, H.D. Betz, On the series of +CG lightning strokes in dancing sprite events, J. Geophys. Res., Atmos. 123 (2018) 11,030–11,047, https://doi.org/10.1029/2017jd028251.

[10] A.B. Chen, H. Chen, C. Chuang, S.A. Cummer, G. Lu, H. Fang, H. Su, R. Hsu, On negative Sprites and the Polarity Paradox, Geophys. Res. Lett. 46 (2019) 9370–9378, https://doi.org/10.1029/2019gl083804.

[11] J.K. Chou, C.L. Kuo, L.Y. Tsai, A.B. Chen, H.T. Su, R.R. Hsu, S.A. Cummer, J. Li, H.U. Frey, S.B. Mende, Y. Takahashi, L.C. Lee, Gigantic jets with negative and positive polarity streamers, J. Geophys. Res. Space Phys. 115 (2010) A00E45, https://doi.org/10.1029/2009ja014831.

[12] L. Contreras-Vidal, R.G. Sonnenfeld, C.L. da Silva, M.G. McHarg, D. Jensen, J. Harley, L. Taylor, R. Haaland, H. Stenbaek-Nielsen, Relationship between sprite current and morphology, J. Geophys. Res. Space Phys. 126 (2021) e2020JA028930, https://doi.org/10.1029/2020ja028930.

[13] S.A. Cummer, J. Li, F. Han, G. Lu, N. Jaugey, W.A. Lyons, T.E. Nelson, Quantification of the troposphere-to-ionosphere charge transfer in a gigantic jet, Nat. Geosci. 2 (2009) 617–620, https://doi.org/10.1038/ngeo607.

[14] C.F. Enell, E. Arnone, T. Adachi, O. Chanrion, P.T. Verronen, A. Seppälä, T. Neubert, T. Ulich, E. Turunen, Y. Takahashi, R.R. Hsu, Parameterisation of the chemical effect of sprites in the middle atmosphere, Ann. Geophys. 26 (2008) 13–27, https://doi.org/10.5194/angeo-26-13-2008.

[15] F. Gordillo-Vázquez, F. Pérez-Invernón, A review of the impact of transient luminous events on the atmospheric chemistry: past, present, and future, Atmos. Res. 252 (2021) 105432, https://doi.org/10.1016/j.atmosres.2020.105432.

[16] M. Hayakawa, Observation of sprites over the Sea of Japan and conditions for lightning-induced sprites in winter, J. Geophys. Res. 109 (2004) A01312, https://doi.org/10.1029/2003ja009905.

[17] M. Hayakawa, T. Nakamura, D. Iudin, K. Michimoto, T. Suzuki, T. Hanada, T. Shimura, On the fine structure of thunderstorms leading to the generation of sprites and elves: fractal analysis, J. Geophys. Res., Atmos. 110 (2005) D06104, https://doi.org/10.1029/2004jd004545.

[18] Y. Hobara, N. Iwasaki, T. Hayashida, M. Hayakawa, K. Ohta, H. Fukunishi, Interrelation between ELF transients and ionospheric disturbances in association with sprites and elves, Geophys. Res. Lett. 28 (2001) 935–938, https://doi.org/10.1029/2000gl003795.

[19] C.L. Kuo, J.K. Chou, L.Y. Tsai, A.B. Chen, H.T. Su, R.R. Hsu, S.A. Cummer, H.U. Frey, S.B. Mende, Y. Takahashi, L.C. Lee, Discharge processes, electric field, and electron energy in ISUAL-recorded gigantic jets, J. Geophys. Res. Space Phys. 114 (2009) A04314, https://doi.org/10.1029/2008ja013791.

[20] C.L. Kuo, R.R. Hsu, A.B. Chen, H.T. Su, L.C. Lee, S.B. Mende, H.U. Frey, H. Fukunishi, Y. Takahashi, Electric fields and electron energies inferred from the ISUAL recorded sprites, Geophys. Res. Lett. 32 (2005) L19103, https://doi.org/10.1029/2005gl023389.

[21] T.J. Lang, S.A. Cummer, S.A. Rutledge, W.A. Lyons, The meteorology of negative cloud-to-ground lightning strokes with large charge moment changes: implications for negative sprites, J. Geophys. Res., Atmos. 118 (2013) 7886–7896, https://doi.org/10.1002/jgrd.50595.

[22] J. Li, S. Cummer, G. Lu, L. Zigoneanu, Charge moment change and lightning-driven electric fields associated with negative sprites and halos, J. Geophys. Res. Space Phys. 117 (2012) A09310, https://doi.org/10.1029/2012ja017731.
[23] N. Liu, L.D. Boggs, S.A. Cummer, Observation-constrained modeling of the ionospheric impact of negative sprites, Geophys. Res. Lett. 43 (2016) 2365–2373, https://doi.org/10.1002/2016gl068256.
[24] G. Lu, S.A. Cummer, R.J. Blakeslee, S. Weiss, W.H. Beasley, Lightning morphology and impulse charge moment change of high peak current negative strokes, J. Geophys. Res., Atmos. 117 (2012) D04212, https://doi.org/10.1029/2011jd016890.
[25] G. Lu, S.A. Cummer, A.B. Chen, F. Lyu, D. Li, F. Liu, R.R. Hsu, H.T. Su, Analysis of lightning strokes associated with sprites observed by ISUAL in the vicinity of North America, Terr. Atmos. Ocean. Sci. 28 (2017) 583–595, https://doi.org/10.3319/tao.2017.03.31.01.
[26] G. Lu, S.A. Cummer, J. Li, L. Zigoneanu, W.A. Lyons, M.A. Stanley, W. Rison, P.R. Krehbiel, H.E. Edens, R.J. Thomas, W.H. Beasley, S.A. Weiss, R.J. Blakeslee, E.C. Bruning, D.R. MacGorman, T.C. Meyer, K. Palivec, T. Ashcraft, T. Samaras, Coordinated observations of sprites and in-cloud lightning flash structure, J. Geophys. Res., Atmos. 118 (2013) 6607–6632, https://doi.org/10.1002/jgrd.50459.
[27] G. Lu, S.A. Cummer, Y. Tian, H. Zhang, F. Lyu, T. Wang, M.A. Stanley, J. Yang, W.A. Lyons, Sprite produced by consecutive impulse charge transfers following a negative stroke: observation and simulation, J. Geophys. Res., Atmos. 121 (2016) 4082–4092, https://doi.org/10.1002/2015jd024644.
[28] G. Lu, B. Yu, S.A. Cummer, K. Peng, A.B. Chen, F. Lyu, X. Xue, F. Liu, R. Hsu, H. Su, On the causative strokes of halos observed by ISUAL in the vicinity of North America, Geophys. Res. Lett. 45 (2018) 10,781–10,789, https://doi.org/10.1029/2018gl079594.
[29] W.A. Lyons, Characteristics of luminous structures in the stratosphere above thunderstorms as imaged by low-light video, Geophys. Res. Lett. 21 (1994) 875–878, https://doi.org/10.1029/94gl00560.
[30] W.A. Lyons, Sprite observations above the U.S. High Plains in relation to their parent thunderstorm systems, J. Geophys. Res., Atmos. 101 (1996) 29641–29652, https://doi.org/10.1029/96jd01866.
[31] A. Malagón-Romero, F.J. Pérez-Invernón, A. Luque, F.J. Gordillo-Vázquez, Analysis of the spatial nonuniformity of the electric field in spectroscopic diagnostic methods of atmospheric electricity phenomena, J. Geophys. Res., Atmos. 124 (2019) 12356–12370, https://doi.org/10.1029/2019jd030945.
[32] D.C. Mashao, M.J. Kosch, J. Bór, S. Nnadih, The altitude of sprites observed over South Africa, South Afr. J. Sci. 117 (2021) 1–8, https://doi.org/10.17159/sajs.2021/7941.
[33] J. Mlynarczyk, J. Bór, A. Kulak, M. Popek, J. Kubisz, An unusual sequence of sprites followed by a secondary TLE: an analysis of ELF radio measurements and optical observations, J. Geophys. Res. Space Phys. 120 (2015) 2241–2254, https://doi.org/10.1002/2014ja020780.
[34] J.R. Myers, C.B. Sande, A.C. Miller, W.H. Warren, D.A. Tracewell, VizieR Online Data Catalog: SKY2000 Catalog, Version 4 (Myers+ 2002). VizieR Online Data Catalog, http://ui.adsabs.harvard.edu/abs/2001yCat.5109....0M/abstract, 2001.
[35] T. Nakamura, M. Hayakawa, Characteristics of mesopheric sprites in the Hokuriku area and their causative lightning discharges, IEEJ Trans. Power Energy 124 (2004) 1012–1020, https://doi.org/10.1541/ieejpes.124.1012.
[36] V.P. Pasko, U.S. Inan, T.F. Bell, Y.N. Taranenko, Sprites produced by quasi-electrostatic heating and ionization in the lower ionosphere, J. Geophys. Res. Space Phys. 102 (1997) 4529–4561, https://doi.org/10.1029/96ja03528.
[37] V.P. Pasko, U.S. Inan, Y.N. Taranenko, T.F. Bell, Heating, ionization and upward discharges in the mesosphere, due to intense quasi-electrostatic thundercloud fields, Geophys. Res. Lett. 22 (1995) 365–368, https://doi.org/10.1029/95gl00008.
[38] V.P. Pasko, M.A. Stanley, J.D. Mathews, U.S. Inan, T.G. Wood, Electrical discharge from a thundercloud top to the lower ionosphere, Nature 416 (2002) 152–154, https://doi.org/10.1038/416152a.
[39] J. Qin, S. Celestin, V.P. Pasko, Dependence of positive and negative sprite morphology on lightning characteristics and upper atmospheric ambient conditions, J. Geophys. Res. Space Phys. 118 (2013) 2623–2638, https://doi.org/10.1029/2012ja017908.
[40] S.C. Reising, U.S. Inan, T.F. Bell, ELF sferic energy as a proxy indicator for sprite occurrence, Geophys. Res. Lett. 26 (1999) 987–990, https://doi.org/10.1029/1999gl900123.
[41] M. Saito, M. Ishii, F. Fujii, M. Matsui, Seasonal variation of frequency of high current lightning discharges observed by JLDN, IEEJ Trans. Power Energy 132 (2012) 536–541, https://doi.org/10.1541/ieejpes.132.536.
[42] D.D. Sentman, E.M. Wescott, D.L. Osborne, D.L. Hampton, M.J. Heavner, Preliminary results from the Sprites94 Aircraft Campaign: 1. Red sprites, Geophys. Res. Lett. 22 (1995) 1205–1208, https://doi.org/10.1029/95gl00583.
[43] T. Shindo, H. Motoyama, A. Sakai, N. Honma, J. Takami, M. Shimizu, K. Tamura, K. Shinjo, F. Ishikawa, Y. Ueno, M. Ikuta, D. Takahashi, Lightning occurrence characteristics in Japan for 17 years: observation results with lightning location systems of electric power utilities from 1992 to 2008, IEEJ Trans. Electr. Electron. Eng. 7 (2012) 251–257, https://doi.org/10.1002/tee.21725.
[44] D. Siingh, R.P. Singh, A.K. Singh, S. Kumar, M.N. Kulkarni, A.K. Singh, Discharges in the stratosphere and mesosphere, Space Sci. Rev. 169 (2012) 73–121, https://doi.org/10.1007/s11214-012-9906-0.
[45] S. Soula, O. van der Velde, J. Montanya, P. Huet, C. Barthe, J. Bór, Gigantic jets produced by an isolated tropical thunderstorm near Réunion Island, J. Geophys. Res. 116 (2011) D19103, https://doi.org/10.1029/2010jd015581.
[46] M. Stanley, M. Brook, P. Krehbiel, S.A. Cummer, Detection of daytime sprites via a unique sprite ELF signature, Geophys. Res. Lett. 27 (2000) 871–874, https://doi.org/10.1029/1999gl010769.
[47] H. Su, R. Hsu, A.B. Chen, S. Chen, S. Mende, R. Rairden, T. Allin, T. Neubert, Observation of angel sprites, in: Space Weather Study Using Multipoint Techniques. Proceedings of the COSPAR Colloquium, vol. 12, 2002, pp. 289–294.
[48] H.T. Su, R.R. Hsu, A.B. Chen, Y.C. Wang, W.S. Hsiao, W.C. Lai, L.C. Lee, M. Sato, H. Fukunishi, Gigantic jets between a thundercloud and the ionosphere, Nature 423 (2003) 974–976, https://doi.org/10.1038/nature01759.
[49] T. Suzuki, M. Hayakawa, Y. Matsudo, K. Michimoto, How do winter thundercloud systems generate sprite-inducing lightning in the Hokuriku area of Japan?, Geophys. Res. Lett. 33 (2006) L10806, https://doi.org/10.1029/2005gl025433.
[50] T. Suzuki, M. Kamogawa, H. Fujiwara, S. Hayashi, MCS stratiform and convective regions associated with sprites observed from Mt. Fuji, Atmosphere 13 (2022) 1460, https://doi.org/10.3390/atmos13091460.
[51] M.J. Taylor, M.A. Bailey, P.D. Pautet, S.A. Cummer, N. Jaugey, J.N. Thomas, N.N. Solorzano, F. Sao Sabbas, R.H. Holzworth, O. Pinto, N.J. Schuch, Rare measurements of a sprite with halo event driven by a negative lightning discharge over Argentina, Geophys. Res. Lett. 35 (2008) L14812, https://doi.org/10.1029/2008gl033984.
[52] O.A. van der Velde, W.A. Lyons, T.E. Nelson, S.A. Cummer, J. Li, J. Bunnell, Analysis of the first gigantic jet recorded over continental North America, J. Geophys. Res. 112 (2007) D20104, https://doi.org/10.1029/2007jd008575.
[53] E. Wescott, D. Sentman, M. Heavner, D. Hampton, O. Vaughan, Blue Jets: their relationship to lightning and very large hailfall, and their physical mechanisms for their production, J. Atmos. Sol.-Terr. Phys. 60 (1998) 713–724, https://doi.org/10.1016/s1364-6826(98)00018-2.
[54] E.M. Wescott, H.C. Stenbaek-Nielsen, D.D. Sentman, M.J. Heavner, D.R. Moudry, F.T.S. Sabbas, Triangulation of sprites, associated halos and their possible relation to causative lightning and micrometeors, J. Geophys. Res. Space Phys. 106 (2001) 10467–10477, https://doi.org/10.1029/2000ja000182.